Pressure-induced reentrant phase behavior in the poly(*N*-vinyl-2-pyrrolidone)–water system

Thomas Sun and H. E. King, Jr.
Exxon Research and Engineering Company, Corporate Research Science Laboratories, Route 22 East, Clinton Township, Annandale, New Jersey 08801
(Received 20 December 1995; revised manuscript received 19 April 1996)

Phase separation and dynamic light scattering experiments were performed on aqueous solutions of poly(*N*-vinyl-2-pyrrolidone) under high pressure conditions to help elucidate the role that hydrogen bonding plays in the solution behavior of water-soluble polymers. From the pressure-induced phase separation experiments we observe reentrant phase behavior in the pressure-temperature plane at fixed composition. Variation of the phase separation pressure with both composition and molecular weight is also investigated. The concentration dependence on the phase separation pressure is weak and the molecular weight dependence exhibits an approximately $M_w^{-1/2}$ scaling. All this behavior can be explained through a modified Flory-Huggins theory that includes the effect of pressure and temperature on hydrogen bonds and the hydrophobic interactions. We use our data to derive fit parameters for this model and the results suggest that not only does the hydrogen bond weaken at high pressure but hydrophobic interactions increase. Dynamic light scattering (DLS) experiments on solutions within the one-phase region of the phase diagram quantify the influence of changing solvent quality on the polymer's conformation. For dilute solutions, which at ambient temperature and pressure exhibit classic good-solvent behavior, a pressure-induced crossover from good to poor solvent behavior is found. Such measurements are shown to give a measure of A_2, an otherwise difficult to measure property at elevated pressure. Above the overlap concentration, this polymer system exhibits aggregate formation. The autocorrelation spectrum contains two relaxations: a fast relaxation mode associated with the usual cooperative diffusion and a slow relaxation mode associated with internal dynamics of the aggregates. Through DLS experiments in the semidilute regime we show that these two modes merge upon increasing pressure, an effect that is completely reversible. The dispersal of the aggregates under pressure suggests that the aggregates depend strongly on water-mediated hydrogen bonds between monomers. [S1063-651X(96)03409-5]

PACS number(s): 61.25.Hq, 64.75.+g, 87.15.By, 36.20.Ey

I. INTRODUCTION

Aqueous nonionic-polymer systems are, in many ways, peculiar. In contrast to purely hydrocarbon polymer systems, which are reasonably well described by the classical Flory-Huggins theory [1], aqueous polymer systems exhibit many unusual properties. Examples include extraordinarily large second virial coefficients [2], lower critical solution temperatures [3–5], reentrant phase behavior [6,7], and polymer aggregation [8–11]. These unusual, and sometimes useful [2], properties can be attributed to hydrogen bonds. Hydrogen bonds differ from van der Waals bonds in two important respects. First, they are highly directional, bending the bond by as little as 10° from its optimum orientation causes severe weakening of the bond [13,14]. Second, hydrogen bond strengths range from 3.0 to 7.0 kcal/mol [15,16], an order of magnitude higher than typical van der Waals bond strengths ($\approx$0.3 kcal/mol). Indeed, these properties of hydrogen bonds impart to water its unusual properties. In aqueous, polymer solutions there is an additional complication: the hydrocarbon moiety on the polymer chain induces hydrophobic interactions between and within polymer chains [17].

To better understand the properties of water-soluble polymers it is therefore useful to be able to tune the hydrogen bond strength. Commonly this is done by adding denaturing agents to the solution [18,19]. This method, however, has obvious drawbacks in terms of irreversibility, possible cosolvency effects, and solution inhomogeneities. A better way is to apply pressure. As previously mentioned, hydrogen bonds are highly directional. A certain volume is therefore needed to form strong hydrogen bonds. Application of pressure reduces the available volume, thereby weakening the bonds [20–22]. This method of tuning the hydrogen bond strength has none of the drawbacks inherent in using denaturing agents. In this paper we present results obtained from dynamic light scattering and phase separation experiments under high pressure conditions on dilute and semidilute, aqueous solutions of poly(*N*-vinyl-2-pyrrolidone), hereafter referred to as PVP. We chose this polymer because it has a strong hydrogen bond (the amide linkage is well known to be a strong hydrogen bonding unit) and because of the widespread interest in this polymer. It has been extensively studied for both its commercial applications as well as its similarity to biological systems [12,23].

This paper is organized in the following manner. In Sec. II we briefly discuss the experimental techniques and apparatus. In Sec. III A we present experimental data on the phase behavior of PVP. At ambient pressure PVP is completely soluble throughout the liquid range of water over a wide composition range [12]. We find that application of pressure introduces both a lower critical solution temperature (LCST) and an upper critical solution temperature (UCST), which meet at a pressure and temperature of 3.9 kbar and 328 K, respectively. The resulting phase diagram is similar to the hydrophilic-hydrophobic driven reentrant phase behavior seen for protein denaturation [24]. Unlike proteins, the interactions for a linear, random-coil polymer such as PVP are relatively simple to quantify. We use a modified

Flory-Huggins theory that includes pressure and temperature effects on hydrogen bonding and hydrophobicity to account for this reentrant behavior. We also quantify the compositional and molecular weight dependence. In Sec. III B we discuss experimental results on the single-chain behavior through studies of dilute solutions of PVP. This is an example of a light scattering study under high-pressure conditions in which a crossover from good to poor solvent behavior is observed, and we demonstrate that such data can yield second virial coefficients. In Sec. III C we present experimental results on the semidilute properties of PVP in water. Previous studies have shown that although PVP in water is a good solvent system, semidilute solutions display strong aggregation behavior [11]. Since other aqueous polymer systems also display aggregation, a topic of current debate is the question of whether such aggregation is an inherent property or the result of contamination. Through dynamic light scattering we show that the aggregation behavior observed here decreases reversibly under application of pressure. This strongly suggests that the aggregated phase is a thermodynamically stable phase in this system. Concluding remarks are in Sec. IV.

II. EXPERIMENTAL TECHNIQUES

Commercial samples of PVP were purchased from Aldrich and dialyzed. The samples used here have weight average molecular weights (determined by static light scattering) of 10, 49, and 389 kg/mol, with polydispersities (determined by gas permeation chromatography (GPC) of 1.85, 3.24, and 3.56, respectively. Distilled, deionized water was obtained from a Millipore Continental Water Systems unit. The level of impurities from such a system is stated to be 20 parts per 1×10^9. Solutions were prepared gravimetrically with syringe filtered water and allowed to stir overnight. For the dynamic light scattering experiments the solutions were doubly filtered with 0.45- and 0.22-μm Millipore syringe filters into sample capsules (described below) that were initially flushed with water filtered through a 0.10-μm Millipore syringe filter. For the phase separation experiments the samples were injected into clean, dry sample capsules without filtering.

The pressurizing equipment was purchased from Harwood Engineering. The primary elements are an Enerpac hand pump, an intensifier, and a mangenin pressure gauge. The Enerpac hand pump is used to apply pressure (up to 20 000 psi) to the input side of the intensifier. The intensifier provides a 16:1 mechanical multiplication of the pressure due to a difference in piston areas between the input and output sides. A calibrated, mangenin pressure gauge, affixed in parallel with the output side, measures the pressure to within ±35 bar. The pressurizing fluid, a 50%-50% mix of water and ethylene glycol, from the output side is then fed into the optical, high pressure cell. This custom-made, steel pressure cell is rectangular in shape and has a cylindrical cavity into which the sample capsule is placed. There are three sapphire windows placed 90° apart to obtain optical access. The sample capsules are tightly toleranced, specially made (Wilmad Glass), pyrex cylinders that have optical flats fused to the bottom. At the top end is a stainless steel piston that transmits the pressure; an O ring on the piston separates the polymer solution from the pressurizing fluid. To heat and cool the samples, copper heat-exchange plates were affixed to the exterior of the pressure cell along with insulation. For low temperatures, a surrounding mantle of dry nitrogen was also used. Fluid from a Neslab RTE-140D cooler flowed through the copper plates. The temperature was monitored with a thermistor attached to the pressure cell. A comparison of temperatures at this exterior point with those actually measured within the cell indicates an approximately 2 K offset at higher and lower temperatures. We have applied this correction to the data reported here.

The dynamic light scattering experiments were performed with 530.9-nm radiation from a krypton laser and a Brookhaven 9000 correlator. All autocorrelation functions were obtained at $\theta=90°$. The dilute solution field autocorrelation functions were fit to a second cumulant form [25]. These results are consistent with results taken in a standard goniometer setup, thereby confirming homodyne scattering for the high pressure setup. The semidilute solution field autocorrelation functions were fit to a double exponential form. Water viscosities, refractive indices, and densities as a function of pressure were obtained from the literature [26,27]. The phase separation experiments were performed with 632.8-nm radiation from a helium-neon laser transmitted through the sample. The sample was visually observed as the pressure was increased. At the phase separation pressure the sample would suddenly (within ≈35 bar) develop a cloudy appearance. For sample concentrations of 5 mg/ml or above, the sample would look opaque; for lower concentrations the first sign of phase separation would be a sudden increase in the intensity of scattered light. This cloudiness is reversible; the solution clarifies as the pressure was dropped below the separation pressure. Since we were unable to stir the solutions *in situ*, we used a fresh sample to obtain each data point (including the data in the P-T curve). Some data were taken in a diamond anvil cell; the equipment and technique have been previously described [3].

III. EXPERIMENTAL RESULTS AND DISCUSSION

A. Phase behavior of PVP in water under pressure and temperature

At ambient pressure PVP is soluble throughout the liquid range of water [12], but under application of pressure at ambient temperature we find that it phase separates. Figures 1 and 2 show the full pressure-concentration (P-C) and temperature-pressure (T-P) phase behavior of PVP in water. The P-C phase diagrams ($T=298\pm1$ K) show the phase separation pressure to have a weak concentration dependence for higher molecular weights, which gradually increases as the molecular weight is lowered. The T-P phase diagram ($M_w=389$ kg/mol, $c=60$ mg/ml) shows the appearance of a LCST, which decreases as the pressure increases. Ordinarily, the LCST increases sharply with a pressure increase [3]; this is the second example of which we are aware that the LCST decreases. In the first example, poly(ethylene oxide), hereafter PEO, in water [3], it was found that the LSCT weakly decreased with pressure up to some threshold at which point it abruptly declined. For PVP we find that the decline is more gradual and eventually a maximum pressure is achieved after which the phase boundary slope changes sign, causing the system to display an UCST as well.

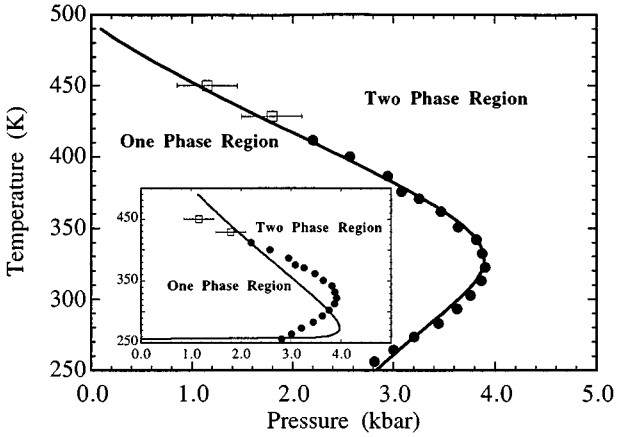

FIG. 1. Phase separation temperatures as a function of pressure for PVP ($M_w = 389$ kg/mol) in water. The solid lines are fit results to the binodal temperatures. The circles are points obtained from the optical cell at $c = 60$ mg/ml; the squares are points obtained from the diamond anvil cell at $c = 250$ mg/ml. The full figure (inset) shows the fit results with (without) a pressure dependence for the hydrophobic interactions. See the text for details.

To analyze these data we use a modified Flory-Huggins theory, developed by Matsuyama and Tanaka [7], to explain the T-C phase behavior of PEO in water. They assume that PEO in water can be considered as a collection of clusters composed of monodisperse polymer chains with varying numbers of water molecules hydrogen bonded to the backbone in a lattice of free water molecules. The free energy per lattice site is given by (setting k_B to unity)

$$\frac{\Delta F_{\mathrm{mix}}}{T} = \phi_0 \ln \phi_0 + \sum_{m=0}^{f} \frac{\phi_{m+1}}{n+m} \ln \phi_{m+1} + \sum_{m=0}^{f} \frac{\phi_{m+1}}{n+m}\left[\frac{\Delta H_{\mathrm{HB}}}{T} - \Delta S_{\mathrm{dis}} - \Delta S_{\mathrm{com}}\right] + \chi\phi(1-\phi), \tag{1}$$

where ϕ_0 is the volume fraction of free water molecules, ϕ_{m+1} is the volume fraction of m clusters (defined as a polymer molecule with m water molecules H bonded to its backbone), ϕ is the total volume fraction of polymer, and n is the number of segments on a polymer molecule. The parameter χ accounts for poor solvent interactions such as hydrophobic interactions and is assumed to change linearly with temperature. The three terms within the square brackets are the enthalpy of water molecules H bonding to the polymer backbone, the change in disorientational entropy upon cluster formation, and the combinatorial entropy. Collectively they represent the change in free energy of cluster formation and are given by

$$\Delta H_{\mathrm{HB}} = -m\Delta\varepsilon,$$
$$\Delta S_{\mathrm{dis}} = \ln\left[\frac{n+m}{n}\left(\frac{\sigma(z-1)^2 w}{ze}\right)^m\right], \tag{2}$$
$$\Delta S_{\mathrm{com}} = \ln\left(\frac{f!}{(f-m)!\,m!}\right),$$

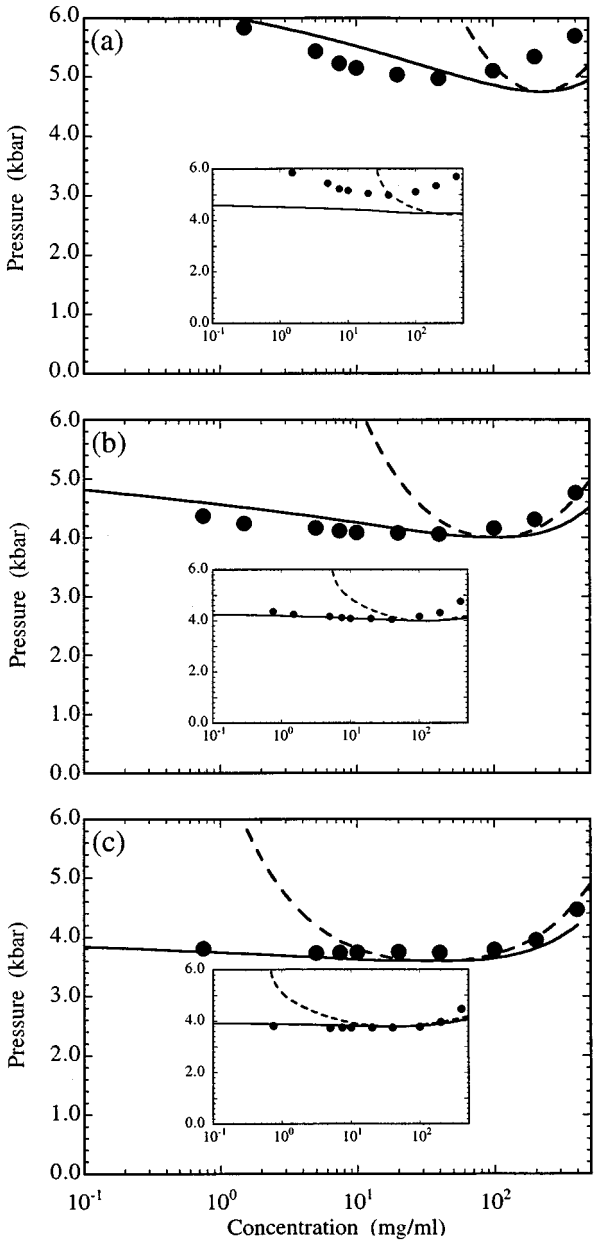

FIG. 2. Phase separation pressures of PVP in water ($T = 298$ K) as a function of molecular weight and concentration. The full figure (inset) shows the fit results with (without) a pressure dependence for the hydrophobic interactions. The solid (dashed) lines are the fit results of the binodal (spinodal) pressures. See the text for details.

where $\Delta\varepsilon$ is the hydrogen bond strength of a single hydrogen bond (defined as a positive quantity), z is the coordination number of the lattice, w is a statistical weight constant, σ is the cluster symmetry number, and f is the number of possible hydrogen bond sites on a polymer chain. This model has been shown to provide a good fit to the reentrant T-C phase behavior of PEO in water. More recently Bekiranov, Bruinsma, and Pincus [28] have shown that the fractional deviations in m about an average value $\overline{m}$ are of order $1/f^{1/2}$ and can therefore be disregarded for large polymer chains. The free energy can then be approximated as

TABLE I. Fitting parameters and uncertainties to the two models.

Fitting parameters	Pressure-independent hydrophobic interactions model	Pressure-dependent hydrophobic interactions model
$\Delta\varepsilon_0$	6866±11123	7823±518
$\ln(\lambda_0)$	−13.6±17.2	−17.8±9.3
A	3.0±1.6	2.0±0.2
B (K^{-1})	$3.8\times10^{-3}\pm6.8\times10^{-3}$	$2.4\times10^{-3}\pm0.5\times10^{-3}$
γ ($kbar^{-1}$)	0.092±0.064	0.038±0.024
α ($kbar^{-1}$)		−0.16±0.03

$$\frac{\Delta F_{\rm mix}}{T}=\phi_0\ln\phi_0+\frac{\phi_{\overline{m}+1}}{\overline{m}+n}\ln\phi_{\overline{m}+1}+\frac{\phi_{\overline{m}+1}}{\overline{m}+n}\left[\frac{-\overline{m}\Delta\varepsilon}{T}-\ln\left(\frac{n+\overline{m}}{n}\lambda_0^{\overline{m}}\right)-\ln\left(\frac{f!}{(f-\overline{m})!\,\overline{m}!}\right)\right]+\chi\phi(1-\phi), \tag{3}$$

where λ_0 is defined as $\sigma(z-1)^2w/ze$ and $\overline{m}(\phi)$ is obtained by minimizing $\Delta F_{\rm mix}$ with respect to m. By assuming $f/n=1$ (as Matsuyama and Tanaka did) and by allowing $\Delta\varepsilon$, λ_0, A, and B to vary (where $\chi=A-BT$), this simplified model also provides good fits to the T-C phase behavior of PEO in water [28].

To fit the T-P-C data for PVP we use the simplified form shown above with modifications to include the effect of pressure on $\Delta F_{\rm mix}$. Although it is known that application of pressure weakens hydrogen bonds, the functional form of the pressure dependence is not known. In the absence of more precise knowledge, we therefore make the simple assumption that the hydrogen bond strength weakens linearly with pressure so that $\Delta\varepsilon(P)=\Delta\varepsilon_0(1-\gamma P)$. By assuming $f/n=1$ and allowing $\Delta\varepsilon_0$, λ_0, A, B, and γ to vary we obtained the fits shown in the insets of Figs. 1 and 2, where the solid (dashed) lines are the binodal (spinodal) pressures and temperatures. The optimum parameters determined through use of a nonlinear least-squares technique are $\Delta\varepsilon_0=6866$ ($\approx 23k_BT$ at $T=298$ K), $\ln(\lambda_0)=-13.6$, $A=3.0$, $B=3.8\times10^{-3}$ K^{-1}, and $\gamma=0.092$ $kbar^{-1}$. These values with the corresponding fitting errors are tabulated in Table I. As can be seen in Fig. 2, this model does an adequate job at describing the P-C behavior at constant temperature. Note, however, that it provides a very poor fit to the T-P phase behavior; it predicts an almost pressure-independent UCST, contrary to what is seen experimentally. The low-molecular-weight concentration scaling of the transition pressure is also poor.

To improve the fits we included a linear pressure dependence to the hydrophobic interactions so that $\chi(T,P)=(A-BT)(1-\alpha P)$. The results of these fits are shown in Figs. 1 and 2. A remarkable improvement in the quality of the fits is found. Both the T-P phase behavior and P-C data are well described. The shape of the binodal pressures as a function of concentration and molecular weight are quite accurate, although the predicted critical concentration for the $M_w=10$ kg/mol sample is somewhat shifted from that observed experimentally. Figure 3 compares the predicted and observed

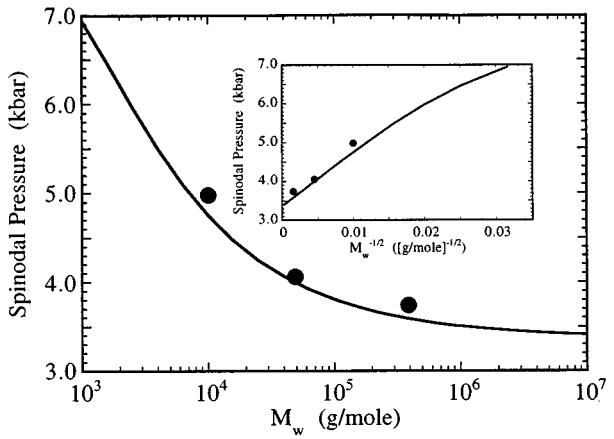

FIG. 3. Molecular weight scaling of the spinodal pressure ($T=298$ K). The solid line is the predicted spinodal pressure at the critical concentration; the circles are experimental data points. The inset shows the spinodal pressure as a function of $M_w^{-1/2}$.

molecular weight scaling of the transition pressure at the critical concentration. As the inset shows, an approximately $(M_w)^{-1/2}$ scaling is obtained. A similar scaling behavior was previously reported for PEO [3]; the present results now suggest that this type of scaling is the result of a nearly linear pressure dependence of the enthalpic contributions to the modified Flory-Huggins theory [1]. The parameters obtained from the fit are $\Delta\varepsilon_0=7823$, $\ln(\lambda_0)=-17.8$, $A=2.0$, $B=2.4\times10^{-3}$ K^{-1}, $\gamma=0.038$ $kbar^{-1}$, and $\alpha=-0.16$ $kbar^{-1}$. The hydrogen bond strength corresponds to 15.5 kcal/mol. This is larger than typical; however, PVP is known to have an exceptionally strong hydrogen bond group and its chemical nature allows two bonds per monomer unit. The resulting γ value suggests an absence of hydrogen bonding at 26 kbar, although the fitting error to this parameter is quite large. For water itself, NMR measurements suggest that it behaves as essentially a hard sphere liquid at about 10 kbar, implying that the hydrogen bond strength has diminished to approximately k_BT by that pressure [20]. The negative value obtained for α implies that the hydrophobic interactions increase with pressure. In support of this conclusion, previous studies on micellar systems [29,30] have shown that the micellar phase region increases with pressure. The authors attribute this to an increase in hydrophobic interactions as pressure is applied. In his book on hydrophobic interactions, Ben-Naim [17] cites various additional experimental evidence that hydrophobic interactions increase with pressure.

From the fitted values, we can now calculate the individual contributions to the free energy at $T=298$ K. These are plotted in Fig. 4 as a function of ϕ at ambient pressure and $P=3.0$ kbar. All experimental work has been done in the $\phi<0.5$ volume fraction region, which corresponds to the concentration range in which the hydrogen bond sites on the chain can be fully saturated, i.e., there is an excess of water. We obtain an interpretation of these terms through Eq. (3). The first two terms describe the mixing entropy associated with combining free water molecules with polymer clusters. It is only weakly pressure dependent. The group of terms within the square brackets of Eq. (3) describes the cluster

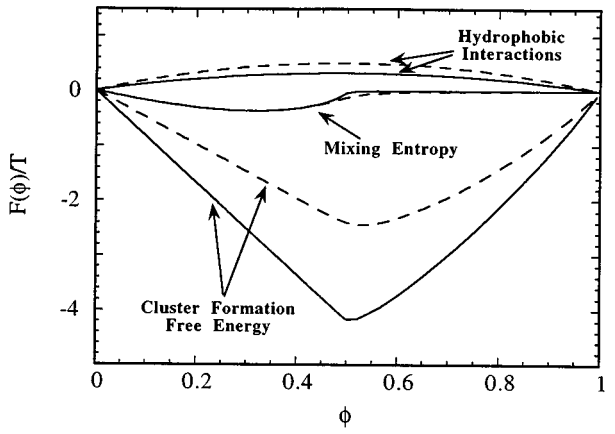

FIG. 4. Various components of the free energy at $T=298$ K [see Eq. (3)]: mixing entropy of clusters and free water molecules, the cluster formation free energy associated with hydrogen bonding, and the hydrophobic interactions. The solid (dashed) lines correspond to ambient pressure ($P=3.0$ kbar).

formation free energy. This energy is strongly pressure dependent and changes by an order of $2k_BT$ in going from ambient to 3.0 kbar. The last term in Eq. (3) describes the hydrophobic interactions. This term is, of course, positive and changes in magnitude by only a fraction of k_BT over the calculated pressure range. As previously noted, the sign of α gives an increased hydrophobic interaction contribution at high pressure.

At this point we should mention that the modified Flory-Huggins theory used above does not include the effect of the volume change upon mixing. At ambient pressure the free energy from this term is negligible. If we assume the volume change upon mixing for PVP in water is the same at 5 kbar as it is ambient pressure [12,31] we find that $P\Delta V_{\mathrm{mix}}$ at 5 kbar pressure is of order of $-1.0k_BT$ with the addition of each monomer unit. Both $\Delta\varepsilon$ and $P\Delta V$ have a linear pressure dependence; hence the latter value can be absorbed in the $\Delta\varepsilon$ value. This would change it little since $\Delta\varepsilon$ is on the order of $\approx 20k_BT$. Another point to consider is sample polydispersity. The effect of polydispersity could best be understood by considering Fig. 3. It shows that the spinodal pressure has a weak molecular weight dependence. If we assume the sample molecular weights to be the weight-average values the model predicts the spinodal pressures to be 4.8, 4.0, and 3.6 kbar for $M=10$, 49, and 389 kg/mol, respectively. If, on the other hand, we assume the sample molecular weights to be the number-average values, the model predicts the spinodal pressures to be 5.2, 4.5, and 3.8 kbar, respectively. These values are not significantly different from the former case. In both cases the predicted spinodal pressures are close to the experimentally observed values of 5.0, 4.1, and 3.7 kbar. We have also fit our data assuming the sample molecular weights to be the number-average values and found that the fitting parameter values change very little from the former case.

B. Dilute solution properties of PVP in water under pressure

The dilute solution properties of a water soluble polymer are determined primarily by a hydrophilic-hydrophobic balance between the hydrogen bond and hydrocarbon moieties of the polymer. PVP has a strong hydrogen bond component that favors solubility, but also a large hydrophobic moiety that favors phase separation. At ambient temperature and pressure the balance between these two energies leads dilute solutions to display typical good solvent behavior [11], with second virial coefficients that are comparable in size to those of prototypical good solvent systems such as polystyrene in toluene [32]. (In contrast, those for PEO in water [2] are a factor of 3 larger, presumably because of the much smaller hydrophobic component for that polymer.) To examine how this changes when the hydrogen bond strength is weakened, we performed a series of dynamic light scattering experiments on aqueous, dilute solutions of PVP under high-pressure conditions. In a dynamic light scattering experiment on a dilute, monodisperse polymer solution the measured diffusion coefficient as a function of concentration is predicted to have the functional form [33,34]

$$D(c)=\frac{k_BT}{6\pi\eta_0R_H}\,(1+k_D^c c+\cdots). \tag{4}$$

Here η_0 is the solvent viscosity and R_H is the hydrodynamic radius. The linear coefficient in the expansion is determined by several thermodynamic and hydrodynamic terms. The predicted relationship is [33]

$$k_D^c=2A_2M-k_S^c-\overline{v}, \tag{5}$$

where A_2 is the second virial coefficient, $\overline{v}$ is the polymer partial specific volume, and k_S^c is the linear term in the concentration expansion for the polymer-solvent friction coefficient

$$f(c)=f_0(1+k_S^c c+\cdots). \tag{6}$$

In a good solvent system A_2 is positive, which enables k_D^c to be positive. The coefficient k_S^c remains positive in both good and θ solvent conditions [1,33]. Hence, in a crossover from good to poor solvent conditions k_D^c decreases and becomes negative as A_2 approaches zero. This predicted behavior is directly observed for PVP as pressure is applied. Figure 5 shows the diffusion coefficients as a function of concentration at pressures ranging from ambient to 3.5 kbar for PVP in water ($M_w=389$ kg/mol). For ease of comparison, all diffusion coefficients in Fig. 5 were normalized to the ambient pressure water viscosity. At ambient pressure $D(c)$ strongly increases with increasing concentration. The slope gradually declines as pressure is applied. At 3.0 kbar pressure $D(c)$ is very nearly concentration independent and at 3.5 kbar pressure $D(c)$ decreases with increasing concentration. To the authors' knowledge, this is the first time a pressure-induced crossover from positive to negative k_D^c values has been observed. In complete contrast, previous work [35] on purely hydrocarbon systems show the polymer solution properties to be pressure independent. The inset in Fig. 5 shows R_H as a function of pressure. Note that in the experimental pressure range R_H decreases from 18.9 to 14.2 nm, another sign of declining solvent quality. The results found here from dynamic light scattering parallel the conclusions drawn from

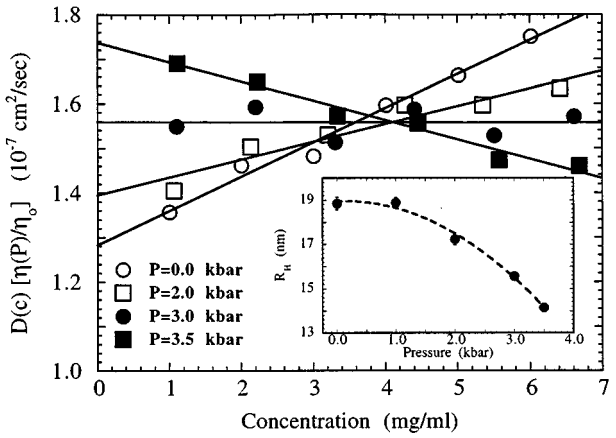

FIG. 5. Normalized diffusion coefficients of PVP ($M_w=389$ kg/mol) in water ($T=298$ K) as a function of concentration at different pressures. Here $\eta(P)$ and η_0 are the viscosities at the experimental and the ambient pressure, respectively. For the sake of clarity, the diffusion coefficients at $P=1.0$ kbar are not plotted. The inset shows R_H as a function of pressure.

intrinsic viscosity measurements of PEO in water [3], in which the viscosity radius R_η decreases from 26 to 16 nm upon application of pressure.

Given k_D^c, Eq. (5) indicates that it should be possible to calculate A_2. This is significant since this important thermodynamic parameter is difficult to measure at high pressures and is rarely reported. We must first calculate k_S^c (we assume $\overline{v}$ to be negligible [34]). Yamakawa [33] predicts the relation

$$k_S^\varphi = 4.8X^3 + 1, \tag{7}$$

where X is defined as

$$X = (3M^2A_2/16\pi N_A R_H{}^3)^{1/3}. \tag{8}$$

Here k_S^φ is the dimensionless form of k_S^c defined as

$$k_S^\varphi = (3M/4\pi N_A R_H{}^3)k_S^c. \tag{9}$$

We can check the validity of this estimate by noting that at ambient pressure $A_2 = 4.7\times10^{-4}$ mol ml/g^2 and near the phase separation pressure (3.75 kbar) A_2 can be assumed to be very close to zero, i.e., $A_2 \approx 0$ at 3.5 kbar. Using Eq. (5), we then calculate k_S^φ at these two pressures as 7.1 and 1.3, respectively. The corresponding values predicted by Eq. (7) are 6.1 and 1.0. This level of agreement leads to a difference of about 30% between the calculated and observed A_2 values at ambient pressure, an acceptable agreement for this otherwise difficult to measure quantity. The values obtained at each pressure are tabulated in Table II. Our results therefore suggest that Yamakawa's relationship along with the measured k_D^c and R_H values can be used to calculate A_2 at pressure from dynamic light scattering (DLS) experiments. An improved estimate might be obtained with a better theoretical calculation of k_S^φ. Cotts and Selser [34] have used a more recent theory by Akcasu [36]; however, this procedure requires that one experimentally fit k_S^φ as a function of X. This is clearly impossible since it requires that A_2 already be known.

TABLE II. Results from dilute solution dynamic light scattering.

Pressure (kbar)	K_D (cm^3/g)	R_H (nm)	$10^4\times A_2$ (mol ml/g^2)
0.0	57.1±3.6	18.9±0.3	3.23
1.0	52.9±4.0	18.9±0.2	3.10
2.0	24.6±3.9	17.2±0.3	1.86
3.0	0.3±2.6	15.6±0.2	0.80
3.5	−24.3±1.7	14.2±0.1	0.19

C. Polymer aggregation under high pressure conditions

Recently it was shown [11] that at concentrations above c^* aqueous PVP solutions exhibit an anomalous slow relaxation mode behavior due to polymer aggregation. Characteristic of this slow mode are a relaxation time that varies as approximately q^3, showing that it is not purely diffusive; strong scattering in the forward direction; a decline in amplitude upon reduction of solvent quality; and a distinct double relaxation in the autocorrelation function (ACF). These features help differentiate it from the slow modes observed in prototypical θ solvent, semidilute hydrocarbon systems. An analysis of the q dependence of the combined static and dynamic light scattering data gave an estimate of the aggregate size of about 100–150 nm, approximately two to three times the radius of gyration of an individual polymer. These aggregates are apparently a thermodynamically stable component of the phase diagram. They coexist in the solutions for long periods of time and can be easily dispersed upon dilution. Note, however, that their presence does not strongly affect the P-C-T behavior. There is no alteration of the transition pressures in Fig. 2 as one passes into the semidilute regime. (Only the $M_w=389$ kg/mol sample would be affected since it has been found that lower molecular weight samples do not exhibit aggregation.)

Data on other nonionic polymers suggest that similar slow mode behavior may be present in other semidilute aqueous systems [8–10], although a complete analysis of both static and dynamic light scattering would be necessary to show that it is due to aggregation. There are reports that even dilute solutions of PEO in water exhibit aggregation [37–39]; this is presently a point of controversy [40]. If aggregation is inherent, one needs to identify an interpolymer interaction that could drive it. For both PVP and PEO a lack of direct monomer-monomer interactions implies some sort of water-mediated interaction. Two possible explanations are that (a) the aggregates are formed by water-mediated hydrogen bonds between polymer molecules (see Fig. 6 in [11]) or (b) given the amphiphilic character of water soluble polymers the aggregates are due to hydrophobic interactions. Without specifying any particular origin for the interactions, de Gennes [41] proposed a qualitative, Flory-Huggins model with a modified enthalpy of mixing in which two monomers repel one another (a good solvent system), but a cluster of monomers can form a stable complex. From this, he showed that at certain polymer concentrations and interaction potentials a good solvent system can exhibit two separate phases. This model was proposed as an explanation of the observed aggregation behavior for PEO. It is distinct from the models

proposed by Matsuyama and Tanaka [7] and Bekiranov, Bruinsma, and Pincus [28], which do not predict polymer aggregation under good solvent conditions.

To better understand the origins of this polymer aggregation, we performed a series of dynamic light scattering experiments on semidilute PVP solutions under pressure. We have previously mentioned that the experimental setup allows scattered light to be obtained only at $\theta=90°$. This is a severe disadvantage in studying polymer aggregation for two reasons. First, the polymer aggregates scatter much more weakly at higher angles; it has been previously been reported [11] that $A_{\text{slow}}/A_{\text{fast}}$ is ≈ 0.5 at $\theta=90°$ as opposed to ≈ 1.75 at $\theta=30°$. This means that the slow component in the ACF at $\theta=90°$ is much less distinct than it would be at lower angles. Second, given that the aggregate radius of gyration is 100–150 nm we find that $qR_g \approx 2.0-3.0$ at $\theta=90°$. Hence the decay of the slow component in the ACF is not due to the diffusive motion of the aggregate as a whole but rather to the internal motions within the aggregate. However, these experiments do address the important issue of whether the polymer aggregation is reversible. In addition, given that application of pressure has opposite effects on hydrogen bond strength and hydrophobic interactions, it is reasonable to suppose that such experiments might differentiate between the relative importance of each in polymer aggregation.

We have already reported [11] that under increasing pressures the slow mode gradually diminishes, essentially disappearing shortly before phase separation and that, more importantly, the ACFs are completely reversible. Here we report the results of fitting the ACF's to the usual [11] double exponential form $g_1(t)=A_{\text{slow}}e^{-\Gamma_s t}+A_{\text{fast}}e^{-\Gamma_f t}$. The inset of Fig. 6 shows the normalized field ACFs for an aqueous, semidilute solution of PVP ($M_w=389$ kg/mol, $c=60$ mg/ml, and $c/c^*\approx 6.0$) at different pressures. At ambient pressure the autocorrelation function, taken within the cell, exhibits a distinct two component relaxation time spectrum. Figures 6(a) and 6(b) show the resulting parameters from the fit: the respective fast and slow relaxation rates and the amplitudes. The larger, open symbols are values obtained from increasing the pressure from ambient to 3.0 kbar. The smaller, solid symbols are values obtained from decreasing the pressure back to ambient. The upright and inverted triangles are values obtained from repressurizing the sample directly to 3.5 kbar pressure. As the pressure increases the slow component amplitude decreases and its decay rate increases; at 3.5 kbar pressure a slow component is not distinctly visible in the autocorrelation function. The fast component relaxation rate decreases by almost an order of magnitude as pressure is applied. This feature is consistent with normal, semidilute behavior when the solvent quality is decreased [42]. These effects are reversible; as the pressure is decreased both the fast and slow components recover to their ambient pressure conditions. Note the nearly complete recovery of the fitted values upon pressure reduction. This is strong evidence that such aggregation is an equilibrium property. Given our predictions for the change in hydrogen bond strength and hydrophobic interactions, the fact that the aggregation declines with pressure indicates that the physical mechanism depends strongly on hydrogen bond mediated linkages and not just hydrophobic interactions.

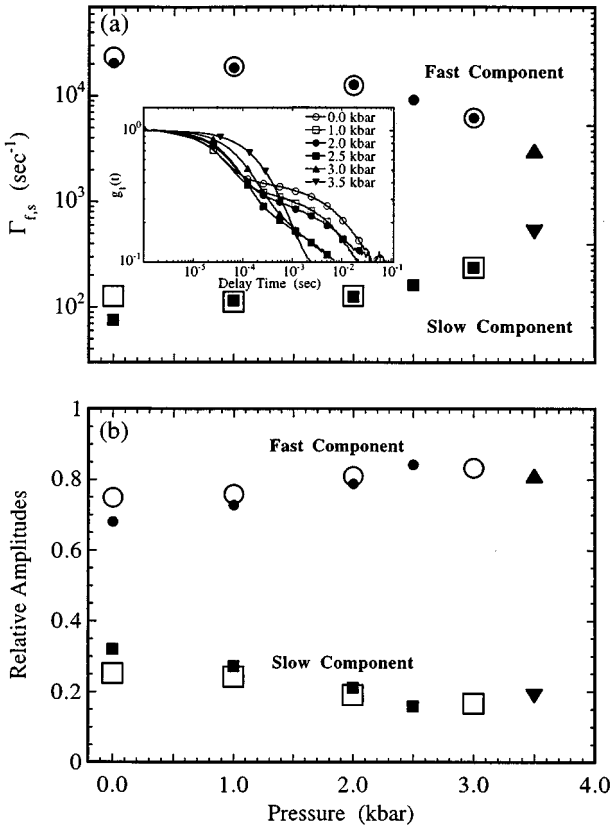

FIG. 6. (a) Decay rates, normalized to ambient pressure viscosity and refractive index, and (b) amplitudes of the fast and slow components obtained from DLS experiments on semidilute, aqueous solutions of PVP ($M_w=389$ kg/mol, $c=60$ mg/ml, and $T=296$ K). The field autocorrelation functions are shown in the inset. The large, open circles and squares are values obtained from the initial pressurization from ambient to 3.0 kbar pressure. The smaller closed circles and squares are values obtained from depressurization back to ambient pressure. The upright and inverted triangles are values obtained from repressurization back to 3.5 kbar. The same sample was used throughout.

IV. CONCLUSION

In conclusion, we have found that the behavior of PVP in water is greatly influenced by pressure, in complete contrast to hydrocarbon systems. In many ways the behavior of PVP in water under pressure mirrors that of PEO [3]. First, we observe the presence of a LCST that decreases as pressure is applied, similar to results found for PEO in water. More interesting, we find that PVP has a reentrant phase behavior, leading to a formerly unknown UCST for this system. We fit this behavior to a modified Flory-Huggins model that includes pressure and temperature effects. The model predicts that reentrant behavior occurs because $\Delta F_{HI}/T$ (or, equivalently, χ in the model) has a linear dependence on pressure and temperature. This linear dependence also leads to an approximate $M_w^{-1/2}$ scaling dependence to the spinodal pressure, also found for PEO in water. Dynamic light scattering results show that PVP in water displays a pressure-driven chain collapse. Intrinsic viscosity measurements for PEO indicate a similar collapse under pressure. DLS experiments on semidilute PVP solutions show that a previously discovered

slow component diminishes reversibly when pressure is applied. These results strongly suggest that the aggregation is inherent and that it depends upon water mediated hydrogen bond linkages, not just hydrophobic interactions. (Preliminary results on aqueous, semidilute PEO solutions indicate a similar behavior.) In closing we find that the pressure effects observed here for PVP arise from pressure-induced changes in hydrogen bonding and hydrophobicity that should be typical for water soluble polymers; hence the pressure effects observed here are very likely inherent to most water soluble polymers.

ACKNOWLEDGMENTS

It is a pleasure to acknowledge D. Herschbach, D. Pine, S. Bekiranov, and P. Pincus for many enlightening conversations. We would also like to express our appreciation to W. Daniels for the loan of the high pressure cell, to L. Wenzel for doing the necessary modifications to the cell, to K. Schug for doing the diamond anvil cell work, to C. Costello for providing the polymer samples, and to K. Colle for providing GPC results.

[1] P. J. Flory, *Principles of Polymer Chemistry* (Cornell University Press, Ithaca, 1953).
[2] K. Devanand and J. C. Selser, Macromolecules **24**, 5943 (1991).
[3] R. L. Cook, H. E. King, Jr., and D. G. Peiffer, Phys. Rev. Lett. **69**, 3072 (1992).
[4] C. A. Finch, in *Polyvinyl Alcohol Developments*, edited by C. A. Finch (Wiley, New York, 1992).
[5] B. Nystrom and R. Bergman, Eur. Polym. **14**, 431 (1978).
[6] S. Saeki, N. Kuwahara, M. Nakata, and M. Kaneko, Polymer **17**, 685 (1976).
[7] A. Matsuyama and F. Tanaka, Phys. Rev. Lett. **65**, 341 (1990).
[8] W. Brown, Macromolecules **17**, 66 (1984).
[9] W. Brown, Polymer **26**, 1647 (1985).
[10] L. Fang and W. Brown, Macromolecules **23**, 3284 (1990).
[11] T. Sun and H. E. King, Jr., Macromolecules **29**, 3175 (1996).
[12] P. Molyneux, *Water-Soluble Synthetic Polymers: Properties and Behavior* (CRC, Boca Raton, FL, 1983), Vol. 1, p. 225.
[13] G. C. Pimentel and A. L. McClellan, *The Hydrogen Bond* (Freeman, San Francisco, 1960), p. 475.
[14] J. S. Walker and C. A. Vause, Sci. Am. **256** (5), 98 (1987).
[15] L. Stryer, *Biochemistry*, 3rd ed. (Freeman, New York, 1988).
[16] F. H. Stillinger, Science **209**, 451 (1980).
[17] A. Ben-Naim, *Hydrophobic Interactions* (Plenum, New York, 1980), p. 311.
[18] F. Franks, in *Water: A Comprehensive Treatise*, edited by F. Franks (Plenum, New York, 1975), Vol. 4, p. 1.
[19] O. Güven and E. Eltan, Makromol. Chem. **182**, 3129 (1981).
[20] J. Jonas, T. Defries, and D. J. Wilbur, J. Chem. Phys. **65**, 582 (1976).
[21] F. H. Stillinger and A. Rahman, J. Chem. Phys. **61**, 4973 (1975).
[22] P. H. Poole, F. Sciortino, T. Grande, H. E. Stanley, and C. A. Angell, Phys. Rev. Lett. **73**, 1632 (1994).
[23] V. Bühler, *Kollidon: Polyvinylpyrrolidone for the Pharmaceutical Industry* (BASF, Ludwigshafen, 1992), p. 285.
[24] K. Heremans, in *High Pressure Chemistry, Biochemistry and Materials Science*, edited by R. Winter and J. Jonas (Kluwer Academic, Boston, 1993), Vol. 401, p. 443.
[25] D. Koppel, J. Chem. Phys. **57**, 4814 (1972).
[26] J. T. R. Watson, R. S. Basu, and J. V. Sengers, J. Phys. Chem. Ref. Data **9**, 1255 (1980).
[27] K. Vedam, CRC Crit. Rev. Solid State Mater. Sci. **11**, 1 (1983).
[28] S. Bekiranov, R. Bruinsma, and P. Pincus (unpublished).
[29] N. Nishikido, N. Yoshimura, and M. Tanaka, J. Colloid Interface Sci. **78**, 338 (1980).
[30] N. Nishikido, J. Colloid Interface Sci. **136**, 401 (1989).
[31] J. Goldfarb and S. Rodriguez, Macromol. Chem. **116**, 96 (1968).
[32] L. J. Fetters, H. Hadjichristidis, J. S. Lindner, and J. W. Mays, J. Phys. Chem. Ref. Data **23**, 619 (1994).
[33] H. Yamakawa, *Modern Theory of Polymer Solutions* (Harper & Row, New York, 1971), p. 419.
[34] P. M. Cotts and J. C. Selser, Macromolecules **23**, 2050 (1990).
[35] R. L. Cook, H. E. King, Jr., and D. G. Peiffer, Macromolecules **25**, 2928 (1992).
[36] A. Z. Akcasu, Polymer **22**, 1169 (1981).
[37] C. Cuniberti and R. Ferrando, Polymer **16**, 306 (1972).
[38] Y. Layec and M. N. Layec-Raphalen, J. Phys. (Paris) Lett. **44**, 121 (1983).
[39] W. F. Polik and W. Burchard, Macromolecules **16**, 978 (1983).
[40] K. Devanand and J. C. Selser, Nature **343**, 739 (1990).
[41] P. G. de Gennes, C. R. Acad. Sci. Ser. 2 **313**, 1117 (1991).
[42] W. Brown and T. Nicolai, in *Dynamic Light Scattering: The Method and Some Applications*, edited by W. Brown (Oxford University Press, New York, 1993), p. 735.